EasyChair Preprint

№ 13120

Active Control of Flow over a Backward-Facing Ramp by Sweeping Jet Actuator

Abderrahim Serrar, Mohamed El Khlifi and Azeddine Kourta

April 28, 2024

Active control of flow over a backward-facing ramp by sweeping jet actuator

A. SERRAR[1*], M. EL KHLIFI[1], A. KOURTA[2]

[1] Hassan II University of Casablanca, Faculty of Sciences and Techniques, BP 146, Mohammedia 28806, Morocco

[2] University of Orléans, INSA-CVL, PRISME, EA 4229, 45072, Orléans, France

*abderrahime.serrare-etu@etu.univh2c.ma

Abstract

This study examines the effects of the sweeping jet actuator on the separated turbulent flow occurring on a backward-facing ramp. The actuator is embedded in the ramp. An unsteady flow analysis has been carried out using 2D Reynolds-Averaged Navier-Stokes equations with a $k-\omega\ SSt$ turbulence model. The effects of the actuator on flow topology and static pressure distribution are analyzed to understand the drag reduction mechanism. The interaction of the oscillating jet, generated by the actuator, with the main flow generates spanwise vortices which is important in transporting the high-momentum flow to the low-momentum separation region, helping to reduce the recirculation length.

Keywords: Backward-facing ramp, Flow control, Sweeping jet actuator.

1. Introduction

Flow on a backward-facing ramp (BFR) separates from the edge of the ramp and attaches further downstream. This is one of the most studied geometries in fluid mechanics. The main reason for this interest is that this geometry exhibits the main characteristics of more complex geometries/separated flows. These include a fixed separation point, a recirculation zone, a reattachment zone and a redeveloping boundary layer [1]. Aerodynamic drag resulting from separation can account for more than 50% of transportation fuel consumption [2]. Various control methods have been envisaged to reduce this drag, and they can be divided into two classes: passive methods, which mainly use geometric or physical characteristics to act on the flow [3], and active methods, which require an external input of energy that must be as low as possible to optimize the ratio of energy supplied to energy gained [4].

Active flow control (AFC) solutions include the sweeping jet actuator (SWJ), which can exhibit highly unsteady spatio-temporal behavior without requiring movements of mechanical elements [5]. Its simple design, robust, and requires low energy input compared to existing AFC systems like synthetic jet [6]. Hence these advantages make it a highly promising technology for a wide range of industrial and aeronautical applications. Koklu and Owens [7], experimentally compared the effects of the installation location of SWJ actuators on separation control, and these actuators installed near the separation point achieved high-pressure recovery. Lim and Lyu [8] carried out an experimental study of a SWJ actuator to control flow separation on an adverse pressure gradient ramp model. An increase in pressure accumulation and a decrease in recirculation length were obtained. Kara et al. [9] numerically studied the effect of adding a SWJ actuator to the surface of a hump to reduce the recirculation length. This actuator generates longitudinal vortex structures that promote mixing between the boundary layer and the stream-flow. The addition of momentum from the outside to the wall increases the energy in the boundary layer, making it more resistant to separation.

The present paper aims to present the effects of a SWJ actuator, on the separated flow over a 2D BFR at a 25^{o} slant angle.

2. Computational method

2.1 Simulation domain

Fig. 1. shows the computational domain with a close-up view of the region near the SWJ actuator. The external flow domain consists on an inclined ramp. Its length is equal to 2.2h with an angle of 25^{o} and connected to two flat plates [2]. The upstream one has a length of 15h. The downstream one has a length equal to 20h. The computational domain includes also the SWJ actuator configuration, where the flow domain is internal. It has two feedback channels, a main chamber, an inlet nozzle, and an outlet nozzle [5].

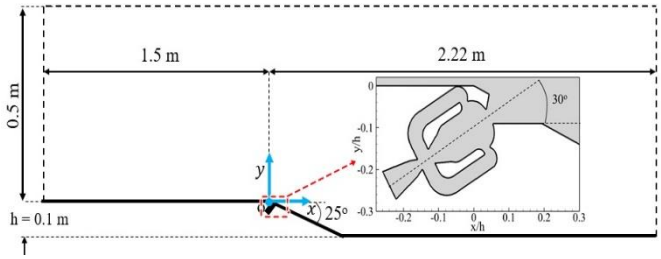

Fig. 1. Computational domain with a close-up view of the region near the SWJ actuator

2.2 Methodology and mesh structure

The ANSYS Fluent CFD software was used for the numerical investigation. The SIMPLE algorithm was used for pressure-velocity coupling for steady-state and unsteady-state calculations. An implicit second-order time discretization was adopted for the unsteady calculation. The

flow equations were discretized by a second-order upwind scheme. Spatial gradients were reconstructed using a least-squares cell-based method. The time step was set at $5x10^{-6}$ s. The working fluid was air. The density was calculated from the ideal gas law. The viscosity was evaluated using Sutherland's law using the reference viscosity μ = 1.8 10^{-5} Pa.s, reference temperature T_{ref} = 288 K [2]. The reference pressure was set to 101,325 Pa. The inlet velocity was U_{ref} = 30 m/s. A fully turbulent flow was assumed. The turbulence intensity at the inlet was 5%, and the turbulent length scale was 1 mm. A convective outflow boundary condition was applied at the outlet. A symmetry condition was adopted for the upper part of the flow domain. A non-slip wall condition has been adopted for the lower part of the flow domain, and the outer and inner walls of the SWJ actuator. A supply pressure equal to 3.5 kPa is imposed at the inlet to the SWJ actuator.

The computational domain is discretized using a hybrid mesh. Most of the computational domain is covered by a triangular mesh, except near the walls, where 16 layers of structured rectangular mesh are generated to capture the flow boundary layer. The height of the first layer of the structured mesh adjacent to the walls is adjusted according to the flow field conditions in order to maintain a y^+ value below unity. The mesh is locally refined in the actuator region and region just outside the outlet of the SWJ actuator. The number of cells is 43.7 10^4.

3. Results and discussion

The BFR is used to test the effectiveness of AFC systems. For this configuration, flow separates at the upper edge of the BFR, resulting downstream in the formation of an extensional recirculation region, a shear layer and a reattachment region [2]. The recirculation region has a length called Lr which is equal to 5.48h according to the following reference [10]. Compared to the experimental PIV results of Kourta et al. [2], good agreement is obtained for the location of the reattachment region downstream of the BFR, with an overestimation of 8.7%. The result is considered acceptable, demonstrating reasonable levels of accuracy and the capabilities of the RANS approaches adopted here.

Fig. 2. shows the evolution of velocity contours superimposed to streamlines inside the SWJ actuator, at 4 different times. The non-dimensional velocity values were obtained by dividing by the reference velocity of U_{ref} = 30 m/s. The main jet is completely attached to the left of the mixing chamber, Fig. 2(a) meanwhile, a large counter-clockwise rotating recirculation bubble exists to the right of the jet. Below the main bubble are two rotating clockwise vortices of varying sizes. It then begins to move from the left to the right wall of the mixing chamber (Fig. 2(b)). This jet is pushed further towards the right wall, where it is completely attached to the right wall of the mixing chamber (Fig. 2(c)). Fig. 2(d) shows that the main jet has detached from the right-hand wall and moved to the left-hand wall of the mixing chamber.

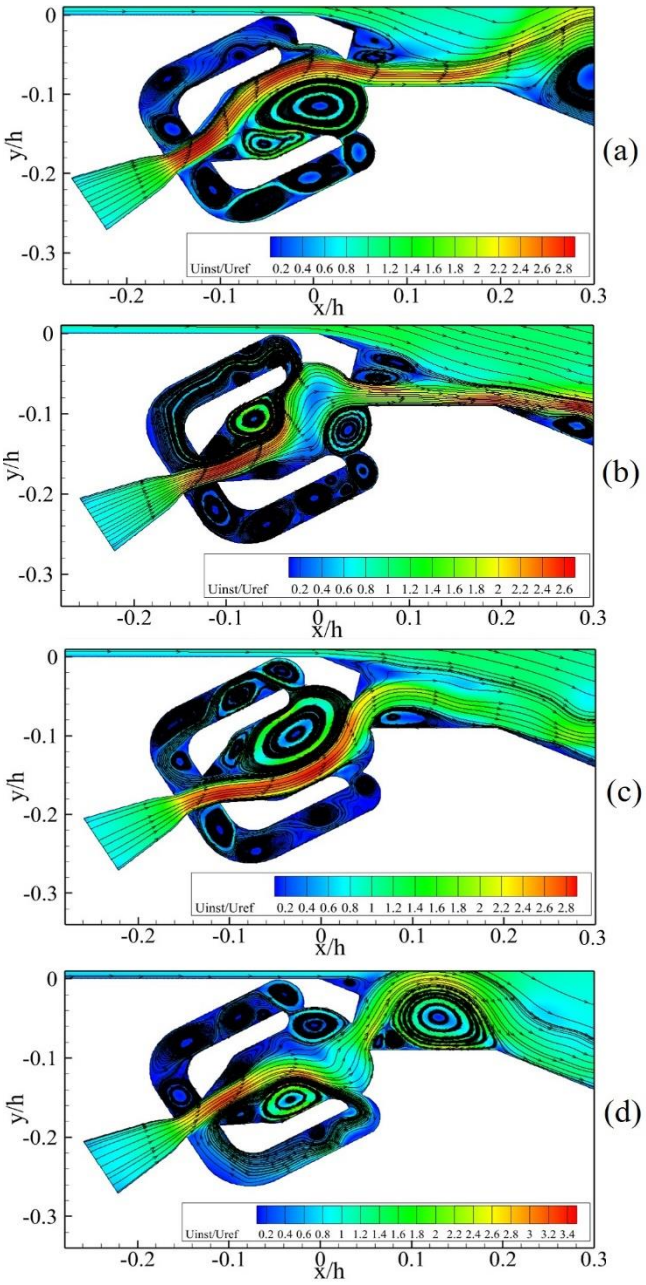

Fig. 2. Evolution of velocity contours superimposed on streamlines inside the SWJ actuator at 4 different times

Fig.3. shows the evolution of velocity contours superimposed to the streamlines at the BFR at four different times. The injection of momentum by the SWJ actuator leads to the creation of vortices of different sizes in the separated shear layer, in contrast to the uncontrolled case where there was only one. The entrainment of fluid towards the boundary layer by these vortices is an important feature, since it makes the resulting boundary layer more resistant to separation.

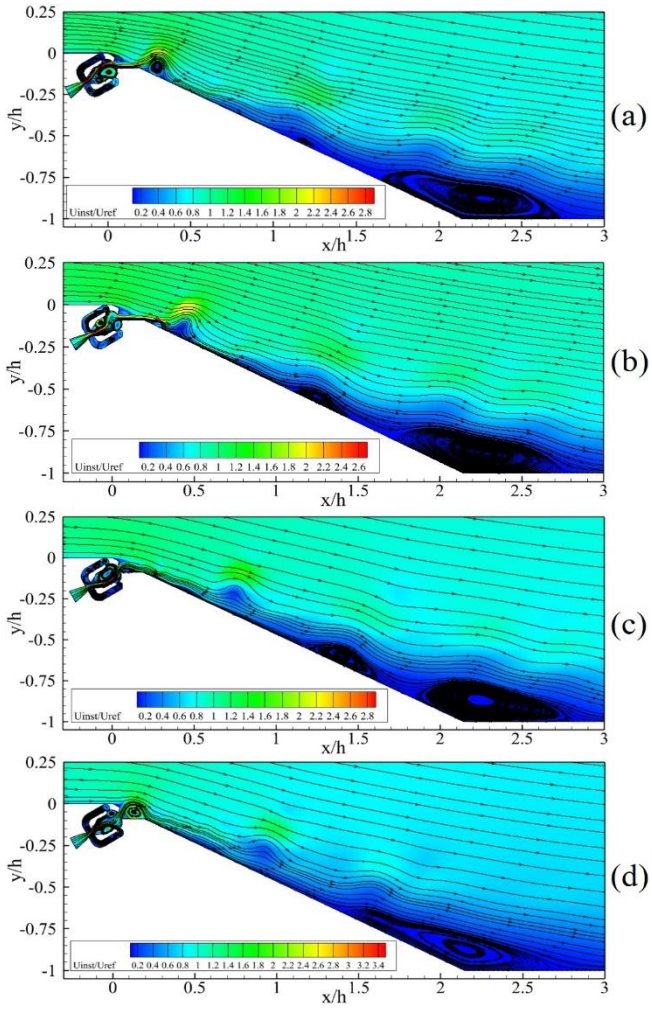

Fig. 3. Evolution of velocity contours superimposed on the streamlines at the ramp at four different times

Fig. 4. shows the velocity contours superimposed to streamlines, time-averaged, at inlet pressure = 3.5 kPa. The dimensionless recirculation length, Lr/h, is reduced by 58.32% compared to the uncontrolled case. The significant reduction in is the result of strong transport of high momentum from the main flow to the low momentum boundary layer.

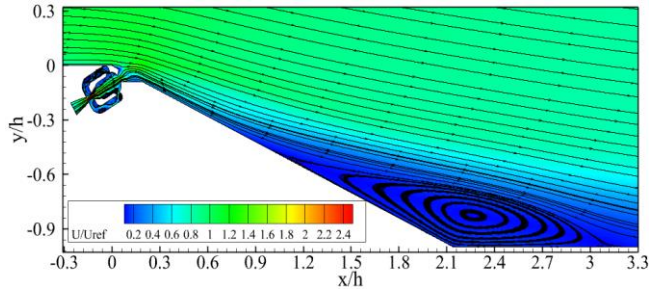

Fig.4. Velocity contours superimposed on streamlines, time-averaged, at inlet pressure = 3.5 kPa

Fig.5. shows a comparison of the pressure coefficient for the uncontrolled and controlled cases. The presence of the SWJ actuator results in a significant increase in pressure recovery and, consequently, a reduction in drag.

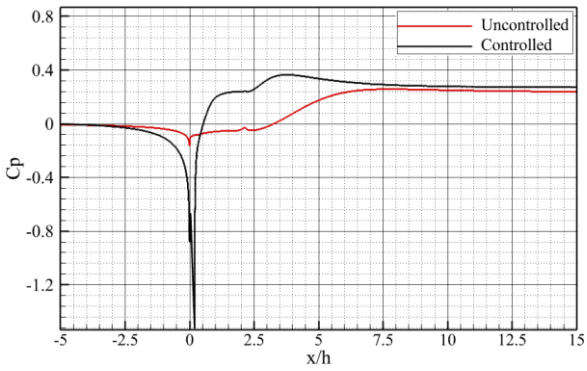

Fig.5. Comparison of pressure coefficient between controlled and uncontrolled cases

4. Conclusion

Simulations were carried out for the 2D backward facing ramp with an integrated SWJ actuator configuration to assess the performance of the sweeping jet actuator compared to the uncontrolled case. A fully turbulent flow was assumed and the $k - \omega\, SST$ turbulence model was used. The sweeping jet actuator is capable of generating vortices which interact with the boundary layer, and play a role in re-energizing the boundary layer by mixing the low momentum fluid near the wall with the energetic fluid of the main flow. In this way, the actuator is able to reattach a separated flow. The reduction in recirculation length is accompanied by an increase in the accumulation of the pressure coefficient, resulting in a reduction in aerodynamic drag.

References

[1] W. Hucho, G. Sovran, *Aerodynamics of road vehicles*, Annual Review of Fluid Mechanics (1993) pp. 485-537.

[2] A. Kourta, T. Adrien, J. Romain, *Analysis and characterization of ramp flow separation*, Experiments in Fluids (2015) pp. 1-14.

[3] H. Park, W. P. Jeon, H. Choi, J. Y. Yoo, *Mixing enhancement behind a backward-facing step using tabs*, Physics of Fluids (2007).

[4] Ceglia. G, Chiatto. M, Greco. C.S, Cardone. G, De Gregorio. F, Cardone. G, de Luca. L, *Active control of separated flow over 2D back-facing ramp by an array of finite-span slotted synthetic jets*, Experimental Thermal and Fluid Science (2021) p. 110475.

[5] A. Serrar, M. El Khlifi, A. Kourta, *Characterisation and comparison of unsteady actuators: a fluidic oscillator and a sweeping jet*, International Journal of Numerical Methods for Heat and Fluid Flow (2022) pp. 1237-1254.

[6] E. Guilmineau, R. Duvigneau, J. Labroquère, *Optimization of jet parameters to control the flow on a ramp*, Comptes Rendus Mecanique (2014) pp. 363-375.

[7] M. Koklu, L. R. Owens, *Flow separation control over a ramp using sweeping jet actuators*, AIAA Paper (2014).

[8] H. D. Lim, Z. Lyu, *Observations of a sweeping jet actuator for flow separation control of a backward-facing ramp*, Physical Review Fluids (2021).

[9] K. Kara, D. Kim, P. J. Morris, *Flow separation control using sweeping jet actuator*, *AIAA Journal* (2018) pp. 1-10.

[10] A. Serrar, *Analyse et contrôle des écoulements turbulents décollés sur une rampe par des oscillateurs fluidiques à jet balayant*, Thèse, Université Hassan II de Casablanca, 2023.